A role for macroautophagy in protection against 4-hydroxytamoxifen–induced cell death and the development of antiestrogen resistance

Julia S. Samaddar,[1] Virgil T. Gaddy,[1] Jennifer Duplantier,[1] Sudharsan Periyasamy Thandavan,[1] Manish Shah,[1] Marlena J. Smith,[1] Darren Browning,[2] Jim Rawson,[3] Sylvia B. Smith,[1] John T. Barrett,[3] and Patricia V. Schoenlein[1]

[1]Departments of Cellular Biology and Anatomy, [2]Biochemistry, and [3]Radiology, Medical College of Georgia, Augusta, Georgia

Abstract

This study identifies macroautophagy as a key mechanism of cell survival in estrogen receptor–positive (ER^+) breast cancer cells undergoing treatment with 4-hydroxytamoxifen (4-OHT). This selective ER modifier is an active metabolite of tamoxifen commonly used for the treatment of breast cancer. Our study provides the following key findings: (*a*) only 20% to 25% of breast cancer cells treated with 4-OHT *in vitro* die via caspase-dependent cell death; more typically, the antiestrogen-treated ER^+ breast cancer cells express increased levels of macroautophagy and are viable; (*b*) 4-OHT–induced cell death, but not 4-OHT–induced macroautophagy, can be blocked by the pan-caspase inhibitor z-VAD-fmk, providing strong evidence that these two outcomes of antiestrogen treatment are not linked in an obligatory manner; (*c*) 4-OHT–resistant cells selected from ER^+ breast cancer cells show an increased ability to undergo antiestrogen-induced macroautophagy without induction of caspase-dependent cell death; and (*d*) 4-OHT, when used in combination with inhibitors of autophagosome function, induces robust, caspase-dependent apoptosis of ER^+, 4-OHT–resistant breast cancer cells. To our knowledge, these studies provide the first evidence that macroautophagy plays a critical role in the development of antiestrogen resistance. We propose that targeting autophagosome function will improve the efficacy of hormonal treatment of ER^+ breast cancer. [Mol Cancer Ther 2008;7(9):2977–87]

Introduction

Breast cancer is one of the leading causes of cancer death in women. For estrogen receptor–positive (ER^+) breast cancers, the prevalent treatment for patients is antiestrogen monotherapy. Tamoxifen is a selective ER modifier and has been the selective ER modifier most commonly used to treat breast cancer. Tamoxifen and newer selective ER modifiers allosterically compete with estradiol (E2) to bind the ER in multiprotein complexes that involve several corepressor proteins (1). In contrast to E2-bound ER, the tamoxifen/ER complex is typically unable to promote tumor growth due to altered gene transcription and nongenomic activities of the ER (2). *In vitro* studies have shown that antiestrogen treatment of breast cancer cells can induce growth arrest (cytostasis) via induction of the cyclin-dependent kinase inhibitors p21 and p27 (3, 4) and cell death (cytotoxicity) by mechanisms still being defined (5–8). These laboratory studies are consistent with the clinical efficacy of antiestrogen therapy that can cause a cessation of tumor growth, increase overall survival (9, 10), and provide chemoprevention (i.e., block the development of ER^+ tumors; refs. 11, 12). Resistance is also a major obstacle to successful therapy with aromatase inhibitors (13, 14), which block E2 production in postmenopausal women and seem to be a more effective therapy than tamoxifen treatment for breast cancer in postmenopausal women (15, 16). Nonetheless, approximately 30% to 50% of women treated with antiestrogen therapy do not initially respond or their breast cancer cells ultimately acquire resistance during treatment (17, 18). Therefore, it is imperative that we understand how antiestrogen resistance occurs in breast cancer patients.

Many studies have been published characterizing the multiple mechanisms of antiestrogen resistance and extensive reviews of this topic are available (13, 14, 19, 20). These studies underscore the involvement of numerous signaling pathways in ER-regulated breast cancer cell growth and suggest novel targets to improve the efficacy of antiestrogen therapy. To date, however, the survival pathway of macroautophagy (also referred to as autophagy) has not been implicated in antiestrogen resistance. Macroautophagy is a catabolic pathway that contributes to normal and cancer cell survival under a variety of stress conditions, including nutrient deprivation (21–24). During macroautophagy, autophagic vesicles are formed. The autophagic vesicles are double membrane-bound vesicles, referred to as autophagosomes and macroautophagosomes, which

Received 7/27/07; revised 5/7/08; accepted 6/7/08.

Grant support: NIH grants CA70897-03 and CA121438.

The costs of publication of this article were defrayed in part by the payment of page charges. This article must therefore be hereby marked *advertisement* in accordance with 18 U.S.C. Section 1734 solely to indicate this fact.

Requests for reprints: Patricia V. Schoenlein, Department of Cellular Biology and Anatomy, Medical College of Georgia, Augusta, GA 30912. Phone: 706-721-3737; Fax: 706-721-6839. E-mail: pschoenl@mail.mcg.edu

doi:10.1158/1535-7163.MCT-08-0447

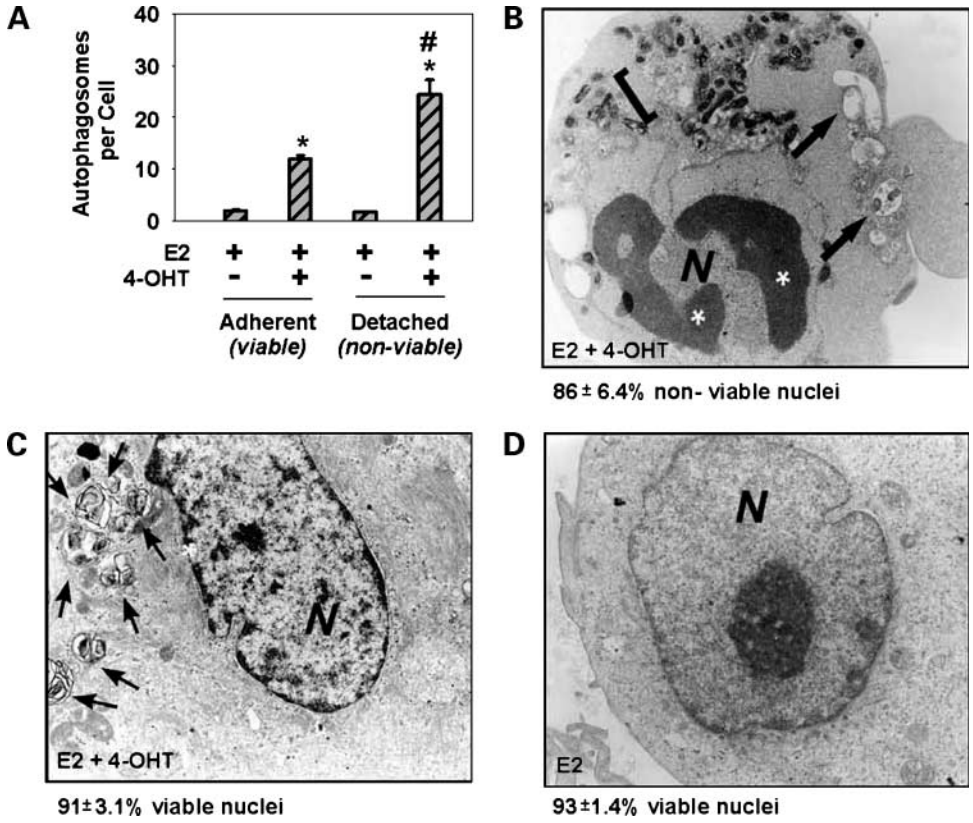

Figure 1. Antiestrogen treatment and the induction of macroautophagy in viable MCF-7 cells. **A,** MCF-7 cells (detached versus adherent) were analyzed for autophagosome levels following treatment with E2 or E2 plus 4-OHT for 72 h. Detached and adherent cells were collected and independently processed for electron microscopic examination. **B** to **D,** nuclear morphology was examined for chromatin compaction in detached, 4-OHT – treated (**B**), adherent, 4-OHT – treated (**C**), and adherent, E2-treated cells (**D**). Irregularly clumped chromatin as seen in **B** is indicative of ACD II. The percentage of nonviable/viable nuclei in detached, 4-OHT – treated (**B**) adherent, 4-OHT – treated (**C**), and adherent, E2-treated (**D**) cell populations is provided at the bottom of each panel. For these experiments, 20 randomly chosen, detached, or adherent cells per treatment were analyzed in three independent experiments in a blind fashion. Statistically significant differences ($P < 0.05$) determined by the Student's *t* test are indicated as follows: *, statistically different compared with E2 treatment group; #, statistically different between the E2 plus 4-OHT treatment groups. Magnifications, ×7,700 (**B**), ×6,000 (**C**), and ×10,000 (**D**). *Arrows,* autophagosome structures; *brackets,* cytosolic area with increased vacuolation; *N,* nucleus; *asterisk,* condensed chromatin.

engulf cytoplasm and/or cytoplasmic organelles and then fuse with lysosomes to degrade the contents of the autophagic vesicle and provide essential building blocks (i.e., amino acids) back to the cell (24, 25). In initial studies in ER^+ breast cancer cells, macroautophagy was appreciated as a tumor suppressor mechanism (26) and precursor to 4-hydroxytamoxifen (4-OHT)-induced autophagocytic cell death [also referred to as active cell death II (ACD II); ref. 27]. However, our past studies have determined that only a small percentage of the population of ER^+ breast cancer cells die in response to antiestrogen therapy; most of the cell population is growth arrested in the G_1 phase of the cell cycle and viable (28, 29). In this study, we tested the hypothesis that 4-OHT induces macroautophagy in ER^+ breast cancer cells that do not die and facilitates the development of antiestrogen resistance. To conduct the study, we primarily used 4-OHT as the antiestrogen treatment and the ER^+ MCF-7 and T-47D breast cancer models. The data generated clearly define a prosurvival role of macroautophagy in ER^+ breast cancer cells and uniquely show that prosurvival role of macroautophagy is critical to the development of acquired 4-OHT resistance.

Materials and Methods

Cell Culture

MCF-7 and T-47D cells were purchased from the American Type Culture Collection. The cells were routinely cultured in DMEM (Atlanta Biologicals) supplemented with 10% fetal bovine serum (FBS; Atlanta Biologicals), 1% L-glutamine (Invitrogen), 2% antibiotics (Invitrogen), and 10 μg/mL insulin (Sigma). Before treatment with E2 (10.0 nmol/L for all experiments) and/or 4-OHT (1.0 μmol/L for MCF-7 and T-47D or 5.0 μmol/L for TR5), cells were cultured in DMEM/F12 medium (Invitrogen) containing 5% dextran-coated charcoal-stripped FBS (DCC FBS; Atlanta Biologicals), which lacks endogenous steroid hormones, 2% antibiotics, and 1% sodium pyruvate (Invitrogen). Cells were grown in 5% CO_2

at 37°C, seeded in triplicate for all experiments, and treated within 24 h of seeding.

Cell Counts

Detached cells were either collected separately or combined with monolayer cells that were released from the culture dish with trypsin treatment. The trypsin was neutralized with 5% DCC FBS DMEM/F12 medium. Cells were then syringed thrice with a 25-gauge needle to obtain single-cell suspensions and counts were done with a hemocytometer. For some experiments, cells were exposed to trypan blue [0.4% trypan blue (Sigma), added to cell suspension for 5 min] to allow the identification of dead cells.

β-Galactosidase Stain

The assay for senescence-associated β-galactosidase was done according to the protocol from Dimri et al. (30). Cells were seeded into chamber slides in DMEM/F12 medium containing E2 or E2 plus 4-OHT, incubated for 36 h, washed twice with PBS, fixed to slides with 2% formaldehyde/0.2% glutaraldehyde for 5 min, and washed with PBS. β-Galactosidase staining solution [1 mg/mL 5-bromo-4-chloro-3-indolyl-β-D-galactopyranoside (5 Prime→3

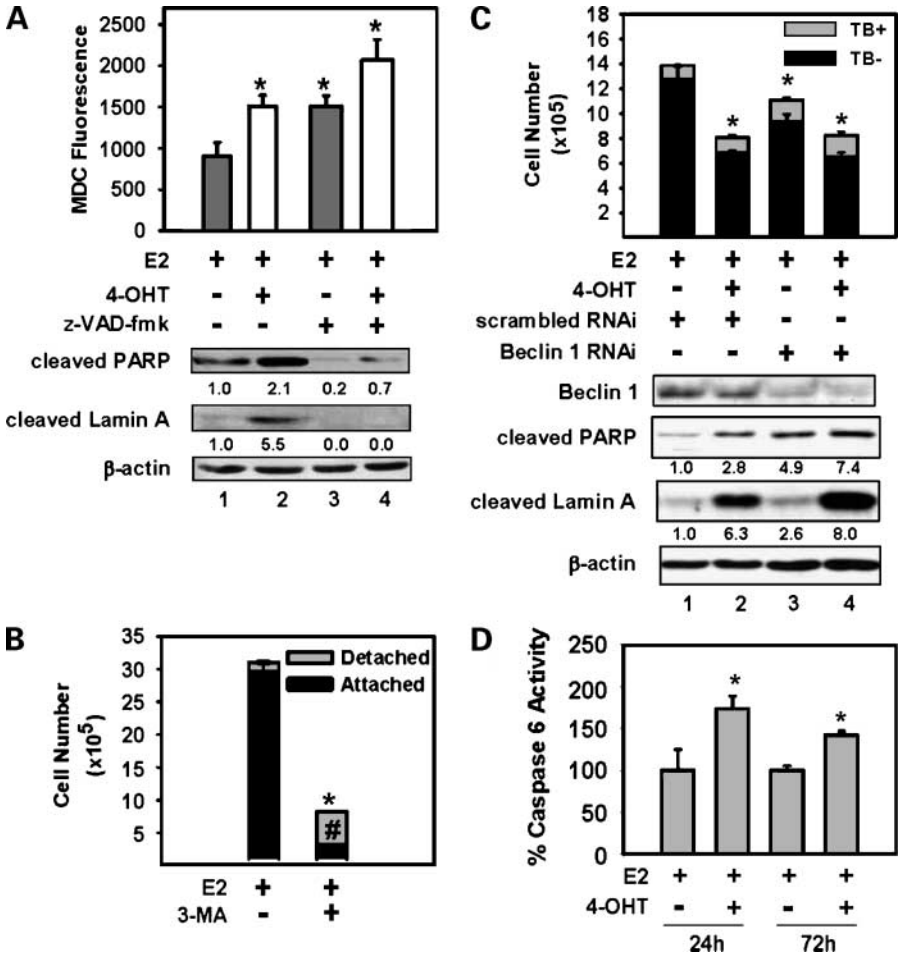

Figure 2. Macroautophagy: a caspase-independent prosurvival response in antiestrogen-sensitive breast cancer cells. **A,** treatment of MCF-7 cells with the pan-caspase inhibitor z-VAD-fmk blocked 4-OHT – induced cleavage of PARP and lamin A but did not inhibit 4-OHT – induced macroautophagy. For these experiments, MCF-7 cells were pretreated with z-VAD-fmk or vehicle (< 0.5% DMSO) for 1 h and then treated for an additional 72 and 96 h with 50 μmol/L z-VAD-fmk with or without E2 or E2 plus 4-OHT. At 72 h of treatment, the MDC sequestration assay was done as detailed in Materials and Methods. At 96 h of hormonal therapy, cells were harvested for protein and analyzed by immunoblotting. **B,** 3-MA treatment induced cell death and blocked autophagosome formation. Cells were treated with or without E2 and 10 mmol/L 3-MA for 120 h; detached (nonviable) and adherent (viable) cells were harvested independently for cell counts in the presence of trypan blue. **C,** Beclin 1 RNAi treatment induced cell death in MCF-7 cells. MCF-7 cells were treated with Beclin 1 RNAi for 48 h followed by treatment with E2 or E2 plus 4-OHT for 96 h. Protein lysates were harvested from the cells and analyzed for levels of Beclin 1, cleaved PARP, and cleaved lamin A. **D,** 4-OHT treatment induced caspase-6 activation. Caspase-6 activity profiles were determined using a commercially available kit according to the manufacturer's instructions (Calbiochem). Cleared lysates were corrected for equal protein concentration using the EZQ Protein Quantitation kit (Molecular Probes, Inc.) and incubated with fluorogenic tetrapeptide substrate Ac-LEHD-AFC for 2 h at 37°C to measure caspase-6 activity levels, respectively. Liberated AFC fluorescence was measured (400 nm excitation, 505 nm emission) using a TECAN microplate fluorometer and software. All experiments were done in triplicate and statistical significance ($P < 0.05$) was determined using the Student's *t* test: *, significance compared with the E2 treatment group; #, significant increase in the number of detached (nonviable) cells following 3-MA treatment.

Prime, Inc.), 40 mmol/L citric acid/sodium phosphate (pH 4.0), 5 mmol/L potassium ferrocyanide (Sigma), 5 mmol/L potassium ferricyanide (Sigma), 150 mmol/L NaCl (Sigma), and 2 mmol/L $MgCl_2$ (Sigma)] was added to the slide and incubated at 37°C. Staining was evident in 4 h and maximal at 12 h.

Cell Harvests, Protein Isolation, Immunoblotting, and Densitometry

Following treatment, cells were collected, centrifuged at 2,000 rpm for 10 min, and resuspended in boiling lysis buffer [5% β-mercaptoethanol (Bio-Rad), 0.12 mol/L Tris (pH 6.8; Fisher Biotech), 20% glycerol (Fisher Biotech), and 4% SDS (Bio-Rad)]. The cell lysate was syringed 20 times with a 18-gauge needle, boiled 5 min, centrifuged at 14,000 rpm for 10 min to pellet cell debris, and subjected to gel SDS-PAGE electrophoresis (50 μg of protein per sample per well). Size-separated proteins were transferred onto polyvinylidene difluoride membrane (Bio-Rad) by electroblotting. Immunoblotting was done as previously described (28, 29). Primary antibodies were used according to the manufacturer's protocol and included Beclin 1 (Santa Cruz Biotechnology), cleaved poly(ADP-ribose) polymerase (PARP; Cell Signaling), cleaved lamin A (Cell Signaling), ERα (Santa Cruz Biotechnology), progesterone receptor (Santa Cruz Biotechnology), LC3 II (Abcam), caspase-3 (Cell Signaling), caspase-9 (Cell Signaling), and β-actin (Sigma). Secondary antibodies included anti-mouse (1:10,000) and anti-rabbit (1:10,000; Jackson ImmunoResearch). Immunodetection was done using the enhanced chemiluminescence (Amersham Pharmacia) detection system and Kodak Scientific Imaging Film (Eastman Kodak Co.). Densitometry was done using a Kodak Digital Science and Kodak Digital Science 1D Image Analysis software (Eastman Kodak Co.). The intensity of β-actin signal was used to correct for variations in protein loading or transfer from gel to membrane. In the figures, the numerical fold difference in intensity of protein signal is provided for each treatment relative to the E2-treated cells unless otherwise specified in the figure legend (number provided below each lane in figure).

Monodansylcadaverine Sequestration Assay

Cells were treated with monodansylcadaverine (MDC; 0.05 mmol/L MDC, diluted in PBS for 30 min) as previously described (31, 32). Following exposure to MDC, the medium with the detached cells was collected and combined with the attached cells that were collected following trypsin treatment. An aliquot of 250,000 cells was pelleted by centrifugation at 2,000 rpm for 10 min. Supernatant was discarded and 400 μL of lysis buffer were added to each pellet. Cells were resuspended in the lysis buffer and incubated on ice with light agitation for 20 min. Lysates were cleared of cell debris by centrifugation at 14,000 rpm for 5 min. The fluorescence of the cleared lysates was determined using a TECAN microplate fluorometer equipped with filters with an emission of 535 nm and an excitation of 340 nm. MDC fluorescence was determined as the mean of three independent experiments for each treatment group and is expressed as the mean ± SE.

LC3-GFP Transfection

Cells to be transfected with the LC3-GFP vector (kindly provided by Dr. Noboru Mizushima) were seeded 24 h before transfection in 5% DCC FBS DMEM/F12 to achieve 70% confluence the day of transfection. Cells were then washed once with HBSS, subjected to trypsin treatment, collected, pelleted by centrifugation (10 min at 1,500 rpm), and resuspended in 400 μL low-serum medium (Opti-MEM; Life Technologies). Five micrograms of LC3-GFP or vector-only DNA were added to the suspension and cells were electroporated (Bio-Rad Gene Pulser Xcell). Following electroporation, cells were seeded in medium containing 10 nmol/L E2, with or without 4-OHT. At 24 to 48 h after transfection, cells were harvested for protein analysis (as described above) or fluorescence microscopy. For fluorescence microscopy, cells were washed with HBSS, fixed with cold methanol for 30 min, washed once with cold acetone and once with PBS, and examined with an Axioplan 2 microscope (Carl Zeiss, Inc.) equipped with an ebq100-isolated epifluorescence condenser. Digital images were captured using a SPOT camera and software (Diagnostic Instruments, Inc.).

Down-regulation of Beclin 1 with RNA Interference

RNA interference (RNAi) technology using RNAi to Beclin 1 (Dharmacon RNA Technologies) was done according to the manufacturer's protocol. Cells were seeded in DMEM/F12 medium containing 5% DCC FBS and insulin (10 μg/mL). Twenty-four hours following seeding, cells were washed and treated with either Beclin 1–targeting RNAi or scrambled RNAi using Oligofectamine (Invitrogen). Forty-eight hours after RNAi treatment, cells were treated with either E2 (10.0 nmol/L) or E2 plus 4-OHT (1.0 μmol/L). At appropriate times, cells were harvested for protein analysis and/or cell counts.

Results

4-OHT–Induced Macroautophagy in Viable MCF-7 Breast Cancer Cells

Studies by Bursch et al. (27) identified antiestrogen-induced MCF-7 cell death as ACD II due to the increased cytosolic levels of autophagosomes and irregularly clumped chromatin in the nuclei of MCF-7 cells undergoing tamoxifen-induced and ICI164 384–induced death. Our past studies have further determined that antiestrogen (4-OHT and ICI 182,780) treatment of MCF-7 cells typically induces cell death in only 20% to 30% of the population (6, 28, 29). The dying cells characteristically detach from the monolayer and show increased levels of high molecular weight DNA fragmentation, cleaved PARP, and cleaved lamin A compared with the adherent, viable monolayer cells (28, 29). Because ~70% of the MCF-7 cell population is not killed by antiestrogen therapy, this study sought to determine if 4-OHT–induced macroautophagy occurs in the surviving, adherent cells as well as the detached, dying 4-OHT–treated cells. Autophagosome number per cell was determined by electron microscopy and determined to be

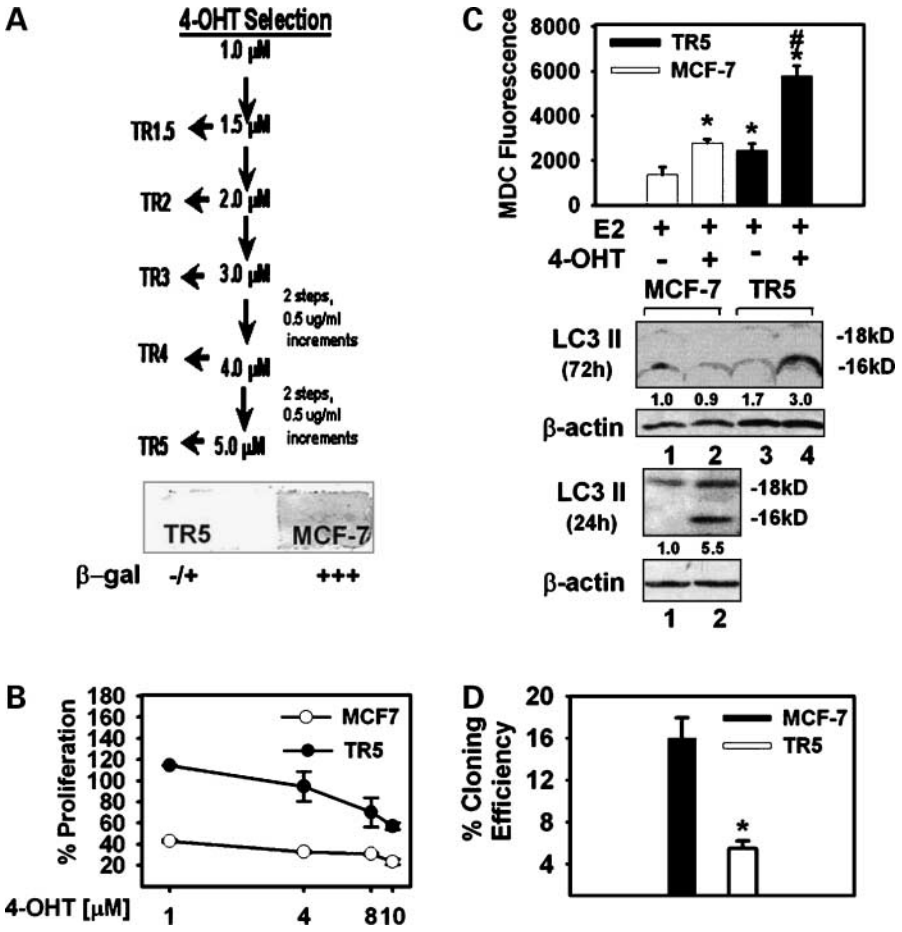

Figure 3. Stepwise 4-OHT selection of MCF-7 cells and the establishment of 4-OHT–resistant sublines with increased autophagosome levels. **A,** stepwise 4-OHT selection used to establish the TR5 subline. Cell populations resistant to cell death induced by 1.5, 2, 3, 4, and 5 μmol/L were designated TR1.5, TR2, TR3, TR4, and TR5, respectively. **B,** a 3-(4,5-dimethylthiazol-2-yl)-2,5-diphenyltetrazolium bromide assay was done as previously described (32) and compared the dose response of TR5 with MCF-7 parent cells at 72 h of treatment with E2 plus varying concentrations of 4-OHT. **C,** high-level MDC sequestration and increased LC3 II (16 kDa) expression were seen in 4-OHT–treated TR5 cells compared with TR5 cells growing in E2 for 72 h or to 4-OHT–treated MCF-7 cells. *, statistically significant increase in MDC sequestration for 4-OHT–treated MCF-7, 4-OHT–treated TR5, and E2-treated TR5 cells compared with the E2-treated MCF-7 cells; #, statistically significant increase in MDC sequestration for 4-OHT–treated TR5 cells compared with 4-OHT–treated MCF-7 cells. **D,** a clonogenic assay showed reduced cloning efficiency of TR5 compared with MCF-7 cells. Cells (300, 500, 1,000, and 1,500) were seeded per 60-mm dish in DMEM/F12 medium with 5% DCC FBS plus E2 in quadruplicate. After 21 d, cells were stained with methylene blue (0.5% in 50% ethanol) and counted. All experiments were done three independent times and statistical significance ($P < 0.05$) was determined using the Student's *t* test.

significantly increased by 4-OHT treatment not only in the detached cells but also in the adherent cell population (Fig. 1A). However, on average, the adherent cells showed fewer autophagosomes per cell. Importantly, >95% of the detached cells treated with 4-OHT showed irregular chromatin condensation in the nucleus, which is typical of a cell dying by ACD II; a representative example is shown in Fig. 1B. In stark contrast, the nuclei of >90% of the adherent, autophagic cells seemed viable (Fig. 1C) and were similar to the nuclei of E2-treated, adherent cells (Fig. 1D). We also determined that in comparison with E2-treated MCF-7 cells, cells seeded without E2 (E2 ablation) also showed higher levels of autophagosomes in viable and nonviable cells (see Supplementary Fig. S1A and B).[4] Treatment with the pure antiestrogen ICI 182,780 also induced macroautophagy concomitant with a reduction in MCF-7 cell number (see Supplementary Fig. S1C and D,[4] respectively). Thus, antiestrogen treatment induced macroautophagy, but it seemed that only the cells with high levels of autophagosomes (>15–20) proceeded to cell death.

A Survival Role For Macroautophagy in ER$^+$ Breast Cancer Cells

We next sought to determine if 4-OHT–induced macroautophagy could be uncoupled from 4-OHT–induced cell death. Because our past studies have shown -OHT–induced caspase activation before 4-OHT induced cleavage of PARP (28) and lamin A (29), we treated MCF-7 cells with the pan-caspase inhibitor z-VAD-fmk to block caspase activity during hormonal therapy. The MDC sequestration assay was used to quantitate macroautophagy and immunoblotting to detect effects on PARP and lamin A. MDC is preferentially sequestered within acidic autophagosomes and has been used in previous studies as an indicator of macroautophagy (31, 32). MDC sequestration was significantly increased (40% increase) in cells treated with E2 plus z-VAD-fmk compared with E2-treated cells. MDC sequestration also was ~25% higher in cells treated with 4-OHT plus z-VAD-fmk compared with 4-OHT treatment alone. Importantly, the apparent increase in macroautophagy corresponded to a decrease in 4-OHT–induced cell death. Detectable levels of cleaved lamin A and cleaved PARP were consistently reduced in hormonal treatment groups containing z-VAD-fmk as shown in Fig. 2A (compare *lanes 3* and *4* with *lanes 1* and *2*). Blockade by z-VAD-fmk of

[4] Supplementary materials for this article are available at Molecular Cancer Therapeutics Online (http://mct.aacrjournals.org/).

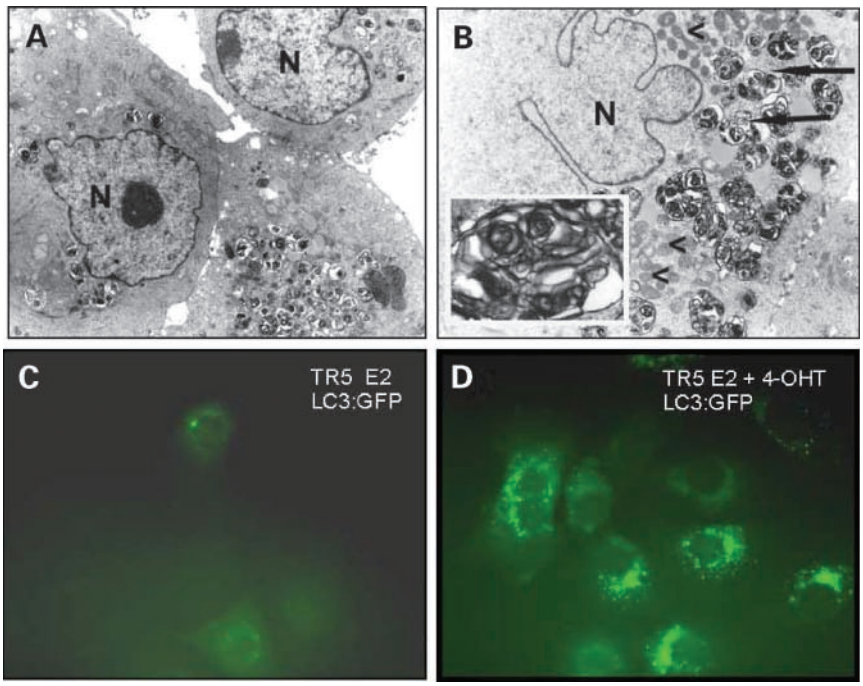

Figure 4. 4-OHT induces macroautophagy in 4-OHT–resistant TR5 cells. **A** and **B,** representative electron micrographs of 4-OHT–treated TR5 cells at ×6,000 and ×12,500, respectively. Examination by electron microscopy determined that the number of autophagosomes per 4-OHT–treated TR5 cell varied, with some cells having high numbers (75 per cell) and some cells having ~10 per cell. The inset is a magnified (×21,500), 4-OHT–induced autophagosome in TR5 cells with lamellated structure indicative of active protein synthesis. *N,* nucleus; *arrows,* autophagosomes. Abundant mitochondria (designated by <) also are evident in the cells. **C** and **D,** LC3-GFP localization studies identified increased autophagosome formation in 4-OHT–treated TR5 cells compared with E2-treated TR5 cells. TR5 cells were transfected (transiently) with LC3-GFP followed by treatment with E2 or E2 plus 4-OHT (5.0 μmol/L). High-level punctate fluorescence of LC3-GFP in **D** is representative of 4-OHT–treated TR5 cells in comparison with E2-treated TR5 cells (**C**) and is consistent with the electron microscopic examination of these antiestrogen-resistant cells.

the basal level of cleaved PARP seen in the E2 treatment group shows that a low level of caspase-dependent cell death occurs in DMEM/F12 medium supplemented with 5% DCC FBS plus E2 by 72 h of MCF-7 growth (Fig. 2A, *lane 3* versus *lane 1*). The z-VAD-fmk–mediated protection from cell death persisted for up to 120 h, at which time neither cell detachment, cleavage of PARP, nor cleavage of lamin A was detected in the 4-OHT–treated MCF-7 cell population (data not shown). These data provide strong evidence that 4-OHT–induced cell death is not an obligatory outcome of 4-OHT–induced macroautophagy.

Because macroautophagy did not seem to be an obligatory precursor to 4-OHT–induced MCF-7 cell death, we wanted to determine if macroautophagy provided a survival role to MCF-7 cells undergoing hormonal therapy. To do this, hormonal treatments were conducted in the presence and absence of 3-methyladenine (3-MA), a small-molecule inhibitor known to block autophagosome formation (33). 3-MA treatment significantly reduced MCF-7 cell number and induced cell death in both E2-supplemented (Fig. 2B) and 4-OHT–supplemented medium (data not shown). A similar sensitivity to 3-MA was shown in T-47D cells, another commonly used ER^+, antiestrogen-sensitive breast cancer model that also undergoes a robust induction of macroautophagy in response to 4-OHT treatment (see Supplementary Fig. S2A–C).[4] These results are in stark contrast to other cell models where 10.0 mmol/L 3-MA blocked cell death because macroautophagy is a prerequisite to ACD II (34, 35). Due to potential off-targeting effects of 3-MA, we also did RNAi targeting of Beclin 1 known to be required for macroautophagy function in MCF-7 cells (26). Targeting Beclin 1 with RNAi effectively reduced Beclin 1 expression by 48 h. At early time points, Beclin 1 reduction in MCF-7 did not significantly affect cell number when compared with the cells treated with nontargeting, scrambled RNAi (data not shown). At later time points (i.e., 168 h), however, a significant reduction in cell number was reproducibly detected in the E2 treatment groups. In addition, increased levels of cleaved lamin A and cleaved PARP were seen in the E2 and the E2 plus 4-OHT treatment groups with RNAi-targeted Beclin 1 down-regulation (Fig. 2C, compare *lanes 3* and *4* with *lanes 1* and 2). Beclin 1 RNAi-induced cell death and reduction in cell number was observed in at least three independent experiments. Because lamin A is specifically cleaved by caspase-6 (36) and our past studies have only identified caspase-9 and caspase-8 activation in 4-OHT–treated MCF-7 cells, we did caspase-6 activity assays and showed a statistically significant 73% increase in caspase-6 by 24 h of 4-OHT treatment and a 42% activation that persisted for at least 72 h (Fig. 2D). Collectively, these data show that 4-OHT induces a caspase-dependent cell death that is more robust if autophagosome formation is blocked by either 3-MA or Beclin 1 down-regulation. Thus, macroautophagy facilitates survival in ER^+ breast cancer cells.

Antiestrogen-Resistant Sublines with an Increased Capacity for Macroautophagy

To determine if macroautophagy-dependent cell survival facilitates the development of antiestrogen resistance, we did a stepwise drug selection in which MCF-7 cells were exposed to small, incremental increases of 4-OHT (Fig. 3A). We chose not to isolate clonal populations of cells because the surviving cells, if undergoing macroautophagy, would most likely be unable to form clones until they fully adapted to the selecting drug concentration. Similar drug selection schemes have been routinely used to isolate

drug-resistant cell lines and identify mechanisms of drug resistance with clinical relevance (37). At each step of 4-OHT selection, cell death occurred in ~20% of the population. The dying cells typically detached from the monolayer, were trypan blue positive, and expressed high levels of cleaved PARP and/or lamin A. Once the cell population adapted to the increased 4-OHT concentration, the population was cryopreserved. The stepwise drug selection was continued until the MCF-7 cell population could sustain viability and proliferate when challenged with 5.0 μmol/L 4-OHT, a concentration of 4-OHT known to accumulate in tissue samples (38, 39). A dose response to 4-OHT for MCF-7 parent cells passaged in E2 for the duration of the selection versus the TR5 cells (4-OHT resistant to 5.0 μmol/L) shows that TR5 cells are completely resistant to the growth inhibitor effects of 1.0 μmol/L 4-OHT (Fig. 3B). In addition, TR5 cells express ER, are not growth stimulated or growth inhibited by E2, do not die in response to 5.0 μmol/L 4-OHT, and can proliferate at this 4-OHT concentration, albeit at a reduced rate (~3-fold slower) than in the absence of 4-OHT (data not shown).

During 4-OHT selection of the TR5 subline, light microscopic examination consistently showed an increase in perinuclear dark granules within the cytosol of the adherent, surviving cells. These granules were not related to senescent granules (30) because β-galactosidase staining, done throughout the selection, showed that the parental MCF-7 cell cytoplasm was consistently more alkaline than that of the resistant cell populations (Fig. 3A). The increased cytosolic acidity of the 4-OHT–selected cells prompted us to examine MDC sequestration in TR5 cells. MDC sequestration was high in 4-OHT–treated TR5 cells but was rapidly lost when 4-OHT treatment was withdrawn; a 64% decrease in MDC sequestration was observed after 72-h growth in E2-supplemented medium (Fig. 3C). In addition, 4-OHT–induced MDC sequestration was 53% higher than in 4-OHT–treated MCF-7 cells. Immunoblotting of protein lysates further showed an increase in the autophagosome-specific 16-kDa lipidated form of LC3 II (40, 41) in 4-OHT–treated TR5 cells compared with E2-treated cells (Fig. 3C). This increase in LC3 II was never observed in MCF-7 cells at this time point (72 h). However, MCF-7 cells routinely showed an increase in the 16-kDa LC3 II from 24 to 36 h of treatment (Fig. 3C, *bottom*). Consistent with the tumor-suppressive effects of macroautophagy (23, 26), TR5 cells were unable to form clones in medium containing 5.0 μmol/L 4-OHT. In contrast, TR5 cells were able to form clones in DMEM/F12 medium containing 5% DCC FBS plus E2, although at a reduced frequency when compared with the cloning efficiency of MCF-7 cells (Fig. 3D).

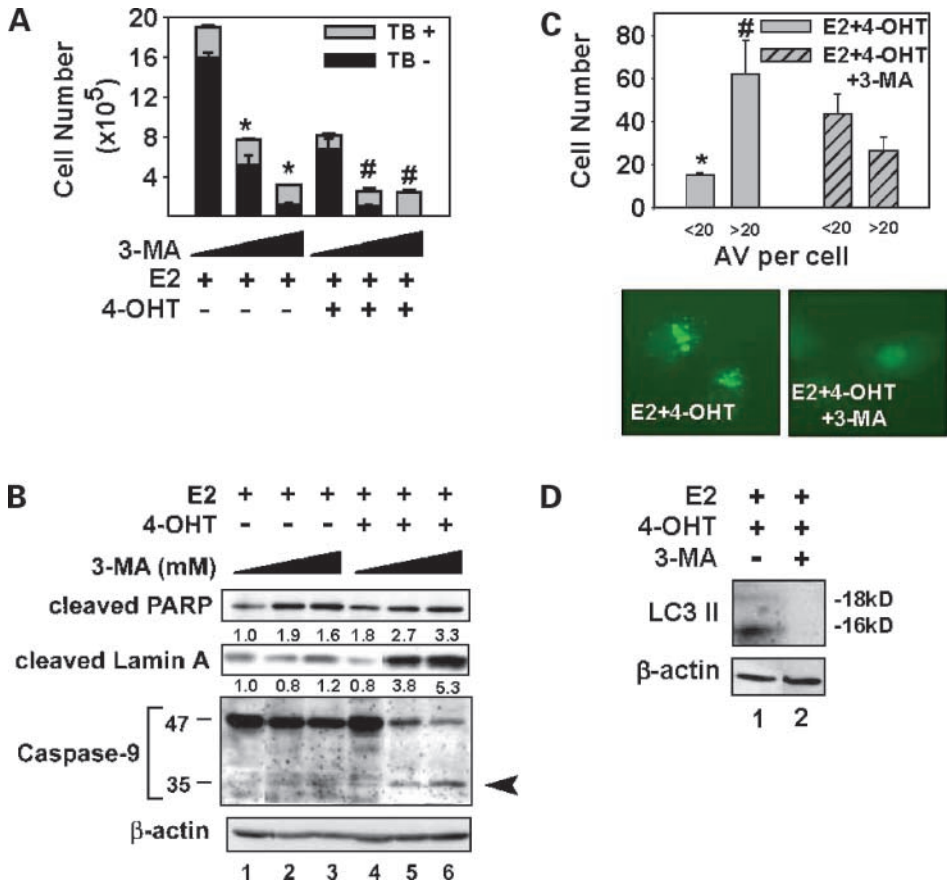

Figure 5. Blockade of autophagosome formation/function in 4-OHT–resistant TR5 cells and the induction of caspase-9 and cell death. **A** and **B,** E2-treated and E2 plus 4-OHT–treated TR5 cells were treated with 0, 5.0, or 10 mmol/L of 3-MA for 168 h to block autophagosome formation/function. Cell counts using trypan blue (*TB*) uptake as a measure of cell death were determined (**A**) and protein isolated from cells was subjected to immunoblotting (**B**). Increased levels of cleaved PARP, cleaved lamin A, and cleaved caspase-9 confirmed 3-MA induction of cell death. **C,** 3-MA treatment reduced autophagosome number in TR5 cells. TR5 cells were transfected with LC3-GFP followed by treatment with E2 or E2 plus 4-OHT for 36 h. Punctate fluorescence of LC3-GFP in TR5 cells was quantified by manual counting of 20 randomly selected cells in two independent experiments. The total number of autophagosomes per cell was decreased in 3-MA–treated TR5 cells. **D,** 3-MA reduced LC3 II (16 kDa) protein in 4-OHT–treated TR5 cells. Protein was isolated from cells treated with E2 plus 4-OHT with or without 3-MA for 48 h and analyzed by immunoblotting.

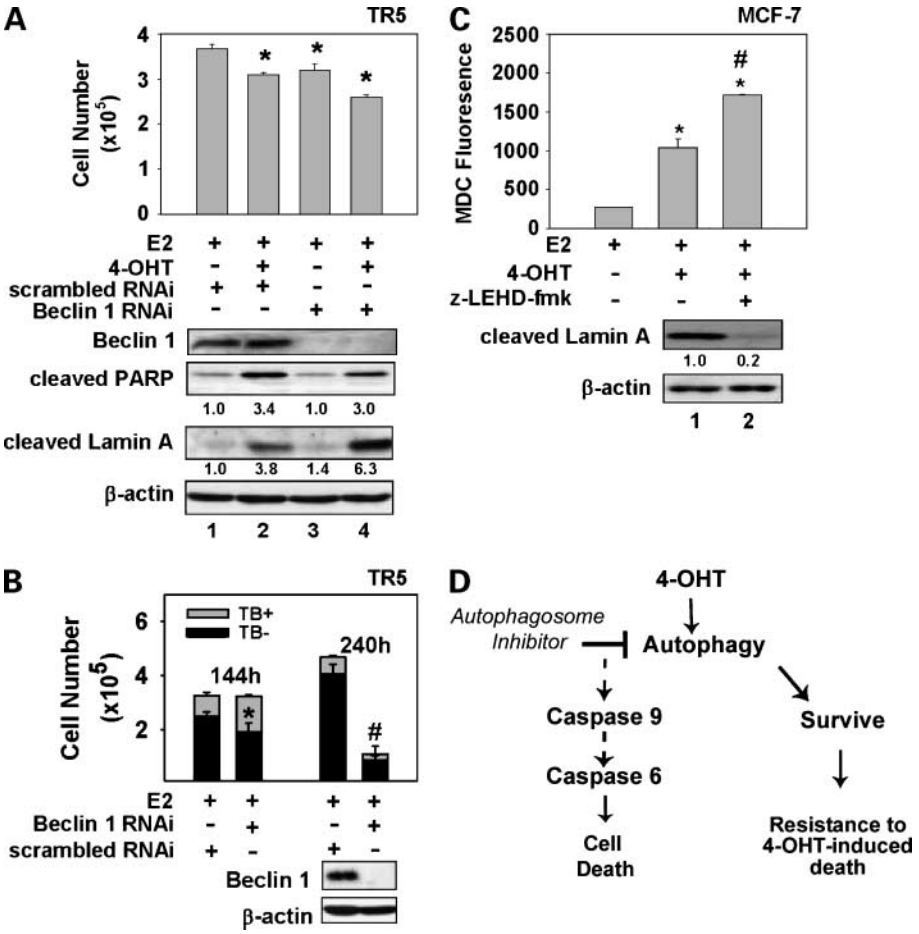

Figure 6. A prosurvival role for autophagosome function in 4-OHT–resistant TR5 cells. **A,** Beclin 1 RNAi targeting in antiestrogen-resistant TR5 cells reduced cell number and induced cell death. At 96 and 144 h of antiestrogen treatment, total cell number was determined and protein lysates were harvested from cells, respectively. Immunoblotting determined that PARP and lamin A cleavage were increased in 4-OHT–treated TR5 cells following Beclin 1 RNAi-mediated knockdown. **B,** TR5 cells were treated with either Beclin 1 RNAi or nontargeting RNAi for 72 h at which time E2 was added to the medium. Cells were harvested at 144 or 240 h for cell counts with trypan blue to determine the ratio of viable versus nonviable cells. Beclin 1 levels were also determined by immunoblotting at 240 h. **C,** caspase-9 inhibition by z-LEHD-fmk enhances MDC sequestration (macroautophagy) and blocks lamin A cleavage. MCF-7 cells were pretreated with vehicle (<0.5% DMSO) or z-LEHD-fmk for 1 h before a 72-h hormonal therapy with or without z-LEHD-fmk (50 μmol/L). Cleaved lamin A levels were reduced by 5-fold when z-LEHD-fmk was present during 4-OHT treatment of cells; signal intensity of 0.2 compared with an arbitrary value of 1.0 in 4-OHT–treated cells. MDC sequestration levels were determined as outlined in Materials and Methods. *Columns,* mean of three independent experiments; *bars,* SE. Statistical significance ($P < 0.05$) was determined using the Student's *t* test: *, statistical significance when compared with E2 treatment; #, significance when compared with E2 plus 4-OHT treatment. **D,** a schematic model in which the blockade of autophagosome function can induce death in the surviving ER^+ breast cancer cell population due to the activation of caspase-9 and caspase-6, which then cleaves lamin A to facilitate nuclear destruction.

Electron microscopic examination confirmed a high evel of autophagosomes in the cytosol of the cells with healthy-appearing nuclei (Fig. 4A and B). In three independent experiments, 50 cells were randomly selected and autophagosome number was determined. The medium number of autophagosomes per 4-OHT–treated TR5 cell was 40, with a range of 10 to 75 per cell. Greater than 90% of the cells with >15 autophagosomes showed healthy-appearing nuclei and many normal mitochondria as seen in the representative cells shown in Fig. 4A and B. This is in stark contrast to MCF-7 cells where high numbers of autophagosomes (>15) were typically present in the detached, dying population of cells (Fig. 1A). Transient transfections with the vector encoding the LC3-GFP fusion protein (40, 41) were also done. Typical punctate staining that accompanies the translocation of LC3 II from the cytosol to the autophagosome membrane was readily detected in 4-OHT–treated TR5 cells (Fig. 4D) and difficult to detect in E2-treated TR5 cells (Fig. 4C). Thus, TR5 cells are uniquely characterized by their ability to transiently sustain high levels of 4-OHT–induced macroautophagy without induction of caspase-dependent cell death.

Blockade of Macroautophagosome Formation/Function Restores 4-OHT Sensitivity to Antiestrogen-Resistant Breast Cancer Cells

To determine if the autophagosomes in TR5 cells provide a survival function, cells were treated with E2 or E2 plus 4-OHT in the presence or absence of 3-MA. 4-OHT plus

3-MA treatment reduced cell number by 73% compared with a 4-OHT–induced 36% reduction (Fig. 5A). The combined treatment (4-OHT plus 3-MA) induced cell death with an overall increase in the number of trypan blue–positive cells (Fig. 5A) and increased cleavage of PARP and/or lamin A (Fig. 5B, compare *lanes 2* and *3* with *lane 1* and *lanes 5* and *6* with *lane 4*). Lamin A cleavage, which was the most obvious marker of cell death in TR5 cells, is mediated by caspase-6 (36), a downstream effector caspase activated by caspase-9. Thus, we further showed that caspase-9 was cleaved to the active 35/37-kDa active form in TR5 cells treated with 4-OHT plus 3-MA (Fig. 5B). TR5 cells treated with 4-OHT monotherapy did not show a significant death response; no induction of lamin A cleavage and only miniscule levels of PARP cleavage were observed (Fig. 5B, compare *lane 4* with *lane 1*), showing their resistance to 4-OHT–induced cell death.

3-MA treatment may induce off-target effects, so we also determined that 3-MA treatment reduced autophagosome number in TR5 cells. TR5 cells treated with 3-MA showed a 40% reduction in cells that contained >20 autophagosomes and a concomitant 75% increase in cells containing <20 autophagosomes per cell (Fig. 5C). Representative photos of cells treated with E2 plus 4-OHT in the presence or absence of 3-MA are shown in Fig. 5C. This reduction in autophagosome number correlated to reduced levels of the 16-kDa LC3 II native protein in total protein lysates following 3-MA treatment of TR5 cells (Fig. 5D). Together, these studies provided strong evidence that 3-MA blocked autophagosome formation in TR5 cells. Similar studies were done with bafilomycin, an agent that blocks autophagosome-lysosome fusion (42). These studies also indicated that loss of autophagosome function was cytotoxic to TR5 cells (see Supplementary Fig. S3).[4]

To further prove that macroautophagy provided a survival function to TR5 cells, RNAi targeting of Beclin 1 in TR5 cells also was done. These studies also showed that loss of autophagosome formation/function resulted in a cytotoxic outcome in antiestrogen-resistant TR5 cells. Beclin 1 reduction via RNAi treatment reduced cell number to 87% in the E2 treatment group and 70% in the E2 plus 4-OHT treatment group compared with the 81% reduction induced by 4-OHT treatment for the same 96-h time interval (Fig. 6A). The reduction in cell number in the 4-OHT–treated cells partly resulted from induction of cell death; cleaved lamin A was reproducibly higher in 4-OHT–treated cells where Beclin 1 was specifically down-regulated (Fig. 6A, compare *lane 2* with *lane 4*). In TR5 cells treated only with E2, the growth-inhibitory and death-inducing effects of Beclin 1 targeting were most obvious at later time points (i.e., Beclin 1 RNAi targeting of TR5 cells growing in E2 and analyzed at 144 and 240 h after treatment; Fig. 6B). Following Beclin 1 knockdown, TR5 cells were fragile and many of the dying cells were degraded before the 240-h harvest shown in Fig. 6B. Although not as robust as the effects of 3-MA or bafilomycin most probably due to a low transfection efficiency of RNAi (approximately 30–50%), the results with Beclin 1 RNAi targeting are consistent with a survival role for the autophagosome in 4-OHT–treated, antiestrogen-resistant TR5 cells. Thus, our working model is that macroautophagosome function contributes to ER^+ breast cancer cell survival and facilitates the development of acquired antiestrogen resistance, whereas blockade of autophagosome formation/function during antiestrogen therapy induces a caspase-9–dependent cell death. From our previous studies, we know that caspase-9 is activated by antiestrogen treatment in MCF-7 cells (28, 29). Thus, we used the caspase-9 inhibitor z-LEHD-fmk to block caspase-9 activation in 4-OHT–treated MCF-7 cells. Blockade of caspase-9 prevented 4-OHT–induced lamin A cleavage, which is needed for nuclear destruction and cell death and significantly increased the autophagocytic response in MCF-7 cells as measured by MDC sequestration (Fig. 6C). In addition, we determined that 4-OHT treatment does not induce caspase-9 activation in TR5 cells (data not shown). These combined data support our working model (schematically depicted in Fig. 6D).

Discussion

In this study, we provide compelling data that macroautophagy induced by 4-OHT plays a critical role in cell survival and facilitates the development of acquired antiestrogen resistance. We have uniquely shown the following: (*a*) 4-OHT treatment increases autophagosome levels in the cytosol of viable ER^+ breast cancer cells, (*b*) 4-OHT–induced macroautophagy can be functionally separated from 4-OHT–induced ACD II, (*c*) macroautophagy facilitates the development of acquired 4-OHT resistance, and (*d*) small-molecule inhibitors of autophagosome formation and function (3-MA and bafilomycin, respectively) and RNAi knockdown of Beclin 1 blocked the growth and induced cell death of antiestrogen-sensitive and antiestrogen-resistant ER^+ breast cancer cells.

Key to this study was the stepwise selection protocol that we used to establish the antiestrogen-resistant TR5 cell population. We reasoned that if breast cancer cells used macroautophagy to escape from 4-OHT–induced death, these autophagocytic cells would be viable but unable to establish clones under 4-OHT selection. This hypothesis was proven in clonogenic assays in which the cloning efficiency of TR5 cells during the drug selections was negligible. However, with 4-OHT withdrawal that consistently leads to a reduction in macroautophagy, clonogenic potential is partially restored to TR5 cells. These data support the stepwise drug selection approach and suggest that clonogenic selections may mask certain contributions of macroautophagy to cell survival and/or lead to the selection of cells that express compensatory mutations that bypass macroautophagy-induced blockade of clonal growth. During this selection, MCF-7 parent cells were passaged in E2 in DMEM/F12 medium for the entire period of TR5 selection and did not show alterations in their response to 4-OHT (data not shown).

Further characterization of TR5 cells is ongoing in our laboratory; however, we are confident in the authenticity of this MCF-7 subline because TR5 cells express ERα and do not express caspase-3 (data not shown), a genotype unique to MCF-7 parental cells and not to other ER^+ breast cancer cell lines (43). We have determined that 4-OHT treatment of TR5 cells is unable to induce caspase-9 or caspase-8 activation (data not shown). These caspases are activated in approximately 20% to 30% of the 4-OHT–treated parent MCF-7 cell (28). Loss of caspase activation in response to 4-OHT treatment but retention of 4-OHT–induced macroautophagy suggests that these two outcomes of 4-OHT treatment are unlinked. Importantly, inhibitors of autophagosome formation and function induced a robust cell death response in TR5 cells, with activation of caspase-9 and cleavage of lamin A as markers of cell death. Thus, the loss of 4-OHT–induced cell death in TR5 cells does not seem to be a general loss of the apoptotic machinery.

The results in this study are in good agreement with the growing recognition of macroautophagy as an antiapoptotic mechanism (22, 24, 44–48). The fact that macroautophagy contributes to cancer cell survival is counterintuitive to the initial, well-described tumor suppressor function of macroautophagy in MCF-7 cells (23, 26). Although in tumor cells, the catabolic process of macroautophagy may be decreased compared with normal cells, it is clear that certain agents and conditions (nutritional starvation) induce macroautophagy before ACD II. As shown in this study and in earlier studies by Bursch et al. (27), 4-OHT induces macroautophagy and ACD II in MCF-7 cells. In this study, we have further shown that cells with the highest numbers of autophagosomes are typically the nonviable cells. However, once caspase activation is blocked with the pan-caspase inhibitor z-VAD-fmk, 4-OHT induces macroautophagy to high levels in cells that do not undergo cell death. These data provide strong evidence that ACD II is not an obligatory outcome of 4-OHT–induced macroautophagy. We propose that the nonviable cells showed higher levels of autophagosomes because these cells were maximally stressed by 4-OHT treatment and macroautophagy was fully induced as a survival mode but failed to rescue the cells. This interpretation would be consistent with the prosurvival role of macroautophagy indicated by our studies with 3-MA treatment, Beclin 1 knockdown, and the 4-OHT selection that generated the TR5 cells. Consistent with a prosurvival role of macroautophagy in breast cancer cell survival, our recent *in vivo* studies with xenografts in nude mice show a high level of autophagosomes in viable tumor cells.[5]

The underlying molecular mechanism of antiestrogen-induced macroautophagy in TR5 cells and several other cell populations that were derived from the stepwise drug selections is currently under investigation in our laboratory. Our emphasis will be to identifying key proteins that may provide new molecular targets to improve the efficacy of tamoxifen therapy. Our data show that Beclin 1 (23, 26) is key to TR5 cell survival. Whether Beclin 1 expression facilitates survival in human breast cancer cells during antiestrogen challenge is an important question and remains to be determined. We plan to dissect the macroautophagy survival pathway in ER^+ breast cancer cells with a focus on the enhanced autophagocytic capacity of TR5 cells.

Overall, our data support a key survival role for macroautophagy that facilitates the progression of a breast cancer cell to antiestrogen resistance. To our knowledge, our studies are the first report linking macroautophagy to the development of antiestrogen resistance. Our studies are in complete agreement with two recent studies (49, 50) in which macroautophagy was shown to reduce the efficacy of chemotherapy and tamoxifen therapy, respectively, in ER^+ breast cancer cells. These combined studies underscore a growing recognition that alterations in the autophagocytic compartment are linked to carcinogenesis and resistance to chemotherapy. Thus, targeting the autophagocytic pathways may provide a new mechanism of anticancer therapy in general. More specifically, we propose that blocking autophagosome function in breast cancer cells undergoing antiestrogen therapy will specifically increase the cytotoxicity of hormonal therapy and reduce the emergence of antiestrogen resistance.

Disclosure of Potential Conflicts of Interest

No potential conflicts of interest were disclosed.

Acknowledgments

We thank Dr. Noboru Mizushima for providing the pEGFP-LC3 plasmid that we have designated LC3-GFP in this manuscript, Insil Kim and Jennifer Cannon for helping with the initial 4-OHT selection, Hutch Jackson for expert technical assistance, and the Horse Barrel Association of Augusta, GA who provided financial support for the initial aspects of this project.

References

1. Jordan VC. Chemoprevention of breast cancer with selective oestrogen-receptor modulators. Nature 2007;7:46–53.

2. Osborne CK, Schiff R. Estrogen-receptor biology: continuing progress and therapeutic implications. J Clin Oncol 2005;23:1616–22.

3. Caldon CE, Daly RJ, Sutherland RL, et al. Cell cycle control in breast cancer cells. J Cell Biochem 2006;97:261–74.

4. Sutherland RL, Musgrove EA. Cyclins and breast cancer. J Mammary Gland Biol Neoplasia 2004;9:95–104.

5. Bouker KB, Skaar TC, Fernandez DR, et al. Interferon regulatory factor-1 mediates the proapoptotic but not cell cycle arrest effects of the steroidal antiestrogen ICI 182,780 (faslodex, fulvestrant). Cancer Res 2004;64:4030–39.

6. El Etreby MF, Liang Y, Wrenn RW, et al. Additive effect of mifepristone and 4-hydroxytamoxifen on apoptotic pathways in MCF-7 human breast cancer cells. Breast Cancer Res Treat 1998;51:149–68.

7. Thiantanawat A, Long BJ, Brodie AM. Signaling pathways of apoptosis activated by aromatase inhibitors and antiestrogens. Cancer Res 2003;63:8037–50.

8. Kallio A, Zheng A, Dahllund J, et al. Role of mitochondria in tamoxifen-induced rapid death of MCF-7 breast cancer cells. Apoptosis 2005;10:1395–410.

9. Early Breast Cancer Trialists' Collaborative Group. Tamoxifen for early breast cancer: an overview of the randomized trials. Lancet 1998;351:1451–67.

[5] P.V. Schoenlein et al., in preparation.

10. Early Breast Cancer Trialists' Collaborative Group. Systemic treatment of early breast cancer by hormonal, cytotoxic, or immune therapy. Lancet 1992;399:1 – 15.

11. Fisher B, Costantino JP, Wickerham DL, et al. Tamoxifen for prevention of breast cancer: report of the National Surgical Adjuvant Breast and Bowel Project P-1 Study. J Natl Cancer Inst 1998;90:1371 – 88.

12. Veronesi U, Maisonneuve P, Rotmensz N, et al. Italian randomized trial among women with hysterectomy: tamoxifen and hormone-dependent breast cancer in high risk women. J Natl Cancer Inst 2003;95:160 – 5.

13. Normanno N, DiMaio M, DeMaio E, et al. Mechanisms of endocrine resistance and novel therapeutic strategies in breast cancer. Endocrine Related Cancer 2005;12:721 – 47.

14. Miller WR, Bartlett JMS, Canney, et al. Hormonal therapy for postmenopausal breast cancer: the science of sequencing. Breast Cancer Res Treat 2007;103:149 – 60.

15. ATAC Trialist's Group. Results of the ATAC (Arimidex, Tamoxifen, Alone or in Combination) trial after completion of 5 years' adjuvant treatment for breast cancer. Lancet 2005;365:60 – 2.

16. BIG1-98 Collaborative Group. A comparison of letrozole with tamoxifen in postmenopausal women with early breast cancer. N Engl J Med 2005;353:2747 – 57.

17. Clarke R, Leonessa F, Welch JN, et al. Cellular and molecular pharmacology of antiestrogen action and resistance. Pharmacol Rev 2001;53:25 – 71.

18. Ariazi EA, Ariazi JL, Cordera F, et al. Estrogen receptors as therapeutic targets in breast cancer. Curr Top Med Chem 2006;6:181 – 202.

19. Nicholson RI, Johnston SR. Endocrine therapy, current benefits and limitations. Breast Cancer Res Treat 2005;93:S3 – 10.

20. Perey L, Paridaens R, Hawle H, et al. Clinical benefit of fulvestrant in postmenopausal women with advanced breast cancer and primary or acquired resistance to aromatase inhibitors: final results of phase II Swiss Group for Clinical Cancer Research Trial (SAKK21/00). Ann Oncol 2007;18:64 – 9.

21. Klionsky DJ, Emr SD. Autophagy as a regulated pathway of cellular degradation. Science 2000;290:1717 – 21.

22. Lum JJ, Bauer DE, Kong M, et al. Growth factor regulation of autophagy and cell survival in the absence of apoptosis. Cell 2005;120:237 – 48.

23. Levine B. Cell biology: autophagy and cancer. Nature 2007;12:745 – 7.

24. Codogno P. Autophagy in cell survival and death. J Soc Biol 2005;199:233 – 41.

25. Debnath J, Baehrecke EH, Kroemer G. Does autophagy contribute to cell death? Autophagy 2005;1:66 – 74.

26. Liang XH, Jackson S, Seaman M, et al. Induction of autophagy and inhibition of tumorigenesis of beclin 1. Nature 1999;402:672 – 6.

27. Bursch W, Ellinger A, Kienzl H, et al. Active cell death induced by the anti-estrogens tamoxifen and ICI164 384 in human mammary carcinoma cells (MCF-7) in culture: the role of autophagy. Carcinogenesis 1996;17:1595 – 607.

28. Gaddy VT, Barrett JT, Delk JN, Kallab AM, Porter AG, Schoenlein PV. Mifepristone induces growth arrest, caspase activation, and apoptosis of estrogen receptor-expressing, antiestrogen-resistant breast cancer cells. Clin Cancer Res 2004;10:5215 – 25.

29. Schoenlein PV, Hou M, Samaddar JS, et al. Downregulation of retinoblastoma protein is involved in the enhanced cytotoxicity of 4-hydroxytamoxifen plus mifepristone combination therapy versus antiestrogen monotherapy of human breast cancer. Int J Oncol 2007;31:643 – 55.

30. Dimri GP, Lee X, Basile G, et al. A biomarker that identifies senescent human cells in culture and in aging skin *in vivo*. Proc Natl Acad Sci U S A 1995;92:9363 – 7.

31. Biederbick A, Kern HF, Elsasser HP. Monodansylcadaverine (MDC) is a specific *in vivo* marker for autophagic vacuoles. Eur J Cell Biol 1995;66:3 – 14.

32. Munafo DB, Colombo MI. A novel assay to study autophagy: regulation of autophagosome vacuole size by amino acid deprivation. J Cell Sci 2001;114:3619 – 29.

33. Seglen PO, Gordon PB. 3-Methyladenine: specific inhibitor of autophagic/lysosomal protein degradation in isolated rat hepatocytes. Proc Natl Acad Sci U S A 1982;79:1889 – 92.

34. Kuncithapautham K, Rohrer B. Apoptosis and autophagy in photoreceptors exposed to oxidative stress. Autophagy 2007;3:433 – 41.

35. Jia L, Dourmashkin RR, Allen PD, Gray AB, Newland AC, Kelsey SM. Inhibition of autophagy abrogates tumour necrosis factor α induced apoptosis in human T-lymphoblastic leukaemic cells. Br J Haematol 1997;98:673 – 85.

36. Orth K, Chinnaiyan AM, Garg M, Froelich CJ, Dixit VM. The CED-3/ICE-like protease Mch2 is activated during apoptosis and cleaves the death substrate lamin A. J Biol Chem 1996;271:16443 – 6.

37. Schoenlein PV. The role of gene amplification in drug resistance. In: Ozols, RF, Goldstein LJ, editors. Anticancer drug resistance: advances in molecular and clinical research. Norwell (MA): Kluwer Academic Publishers; 1995. pp. 167 – 200.

38. Kisanga ER, Gjerde J, Guerrieri-Gonzaga A, et al. Tamoxifen and metabolite concentrations in serum and breast cancer tissue during three dose regimens in a randomized preoperative trial. Clin Cancer Res 2004;10:2336 – 43.

39. Dragan YP, Fahey S, Nuwaysir E, et al. The effect of tamoxifen and two of its non-isomerizable fixed-ring analogs on multistage rat hepatocarcinogenesis. Carcinogenesis 1996;7:585 – 94.

40. Kabeya Y, Mizushima N, Ueno T, et al. LC3, a mammalian homologue of yeast Apg8, is localized in autophagosome membranes after processing. EMBO J 2000;19:5720 – 8.

41. Mizushima N. Methods for monitoring autophagy. Int J Biochem Cell Biol 2004;36:2491 – 502.

42. Yoshimori T, Yamamoto A, Moriyama Y, et al. Bafilomycin A1, a specific inhibitor of vacuolar-type H^+-ATPase, inhibits acidification and protein degradation in lysosomes of cultured cells. J Biol Chem 1991;266:17707 – 12.

43. Janicke RU, Sprengart ML, Wati MR, et al. Caspase-3 is required for DNA fragmentation and morphological changes associated with apoptosis. J Biol Chem 1998;273:9357 – 60.

44. Paglin S, Hollister T, Delohery T, et al. A novel response of cancer cells to radiation involves autophagy and formation of acidic vesicles. Cancer Res 2001;61:439 – 44.

45. Boya P, Gonzalez-Polo RA, Casares N, et al. Inhibition of macroautophagy triggers apoptosis. Mol Cell Biol 2005;25:1025 – 40.

46. Heymann D. Autophagy: a protective mechanism in response to stress and inflammation. Curr Opin Investig Drugs 2006;7:443 – 50.

47. Sato K, Tsuchihara K, Fujii S, et al. Autophagy is activated in colorectal cancer cells and contributes to the tolerance to nutrient deprivation. Cancer Res 2007;67:9677 – 84.

48. Amaravadi RK, Yu D, Lum JJ, et al. Autophagy inhibition enhances therapy-induced apoptosis in a *MYC*-induced model of lymphoma. J Clin Invest 2007;117:326 – 36.

49. Abedin MJ, Wang D, McDonnell MA, et al. Autophagy delays apoptotic death in breast cancer cells following DNA damage. Cell Death Differ 2005;3:500 – 10.

50. Qadir M, Dwok B, Dragowska WH, et al. Macroautophagy inhibition sensitizes tamoxifen-resistant breast cancer cells and enhances mitochondrial depolarization. Breast Cancer Res Treat. In press 2008.

Molecular Cancer Therapeutics

A role for macroautophagy in protection against 4-hydroxytamoxifen–induced cell death and the development of antiestrogen resistance

Julia S. Samaddar, Virgil T. Gaddy, Jennifer Duplantier, et al.

Mol Cancer Ther 2008;7:2977-2987.